

A novel synthetic derivative of quercetin, 8-trifluoromethyl-3,5,7,3',4'-O-pentamethyl-quercetin, inhibits bladder cancer growth by targeting the AMPK/mTOR signaling pathway

Ting Tao^{1,2}, Caimei He^{1,2}, Jun Deng^{1,2}, Yanjun Huang^{1,2}, Qiongli Su^{1,2}, Mei Peng^{1,2,4}, Meiling Yi^{1,2}, Kwame Oteng Darko^{1,2}, Hui Zou^{1,2} and Xiaoping Yang^{1,2,3}

¹Key Laboratory of Small Targeted Molecules' Discovery, Hunan Normal University, Changsha, Hunan, 410013 China

²Department of Pharmacy, School of Medicine, Hunan Normal University, Changsha, Hunan, 410013 China

³Key Laboratory of Animal Nutrition and Human Health, Hunan Normal University, Changsha, Hunan, 410013 China

⁴Department of Pharmacy, Xiangya Hospital, Central South University, Changsha, Hunan, 410008 China

Correspondence to: Hui Zou, **email:** zouhui308@163.com
Xiaoping Yang, **email:** xiaoping.yang@hunnu.edu.cn

Keywords: 8-Trifluoromethyl-3,5,7,3',4'-O-pentamethyl-quercetin, quercetin, derivative of quercetin, AMPK, mTOR

Received: January 20, 2017

Accepted: April 27, 2017

Published: May 11, 2017

Copyright: Tao et al. This is an open-access article distributed under the terms of the Creative Commons Attribution License 3.0 (CC BY 3.0), which permits unrestricted use, distribution, and reproduction in any medium, provided the original author and source are credited.

ABSTRACT

Quercetin is a naturally existing compound and shows attractive anticancer properties for a variety of solid tumors including glioma, bladder cancer, hepatocellular carcinoma, breast cancer, hematological malignancies and prostate carcinoma. However, these anticancer properties have not been clinically approved due to unclear mechanistic information and its low bioactivity. In our previous study, we elucidated that quercetin activates AMPK pathway which is the major mechanism for its unique anticancer effect in bladder cancer. In the present study, we are trying to enhance its bioactivity by chemical modification using fluorination approach to prepare novel chemical entities, based on the principle of intermediate derivative method (IDM). The compound we obtained is named 8-trifluoromethyl-3,5,7,3',4'-O-pentamethyl-quercetin (TFQ), characterized by NMR spectra and mass spectrum (MS). The results from MTT and cologenic assay in two human and one murine bladder cancer cell lines showed that TFQ exhibits more potent inhibition on the three bladder cancer cell lines than quercetin (Que) although this enhanced effects is not very dramatic. Furthermore, we found that the survival of normal bladder cells PEBC was not significantly suppressed by TFQ compared with Que. Western blot analysis showed that TFQ possess more potent AMPK activation than Que. The downstream of AMPK was further examined by western blot. TFQ treatment is able to inactivate mTOR signaling pathway with the regulation of mTOR, 4EBP1 and P70S6K. These results demonstrated that the fluorinated quercetin derivative TFQ inhibits bladder cancer cell growth through the AMPK/mTOR pathway. Altogether, our findings suggest that TFQ could serve as a new potential therapeutic agent for bladder cancer more effective than Que.

INTRODUCTION

Bladder cancer is the fifth most common malignancy in United States, with an estimated 76,960 new cases and 16,390 deaths in 2016 [1-2]. Even though transurethral resection has served as the standard treatment, recurrence

and metastasis are often seen in clinic [3]. The commonest way to prevent recurrence and progression is supplemented with intravesical chemotherapy or immunosuppressive agents [4, 5]. Despite these brave efforts, outcomes have changed very little for the past three decades [6]. Metabolism of bladder cancer represents a key issue for

cancer research. Several metabolic altered pathways are involved in bladder tumorigenesis [7].

Quercetin is a naturally existing flavonoid in several vegetables and fruits with attractive biological activities [8]. It has been demonstrated that this small molecule has extensive pharmacological effects, including antitumor, antioxidative and anti-inflammatory activities [9, 10]. The anticancer activity of quercetin has been shown in many kinds of cancers including breast cancer [11, 12], pancreatic cancer [13], medulloblastoma [14], myeloma [15], glioma [16] and bladder cancer [17, 18].

In United States, quercetin has been approved as a non-prescription drug widely used to treat prostate cancer. However, quercetin alone has poor bioavailability [19]. Thus, people have contributed fairly amount of efforts to modify the chemical structure of quercetin for the purpose of obtaining more active compounds via etherification [20], esterification [21], Mannich reaction [22] and metal complexes of quercetin [23, 24]. In a previous study, we reported the synthesis of brominated quercetin derivatives [25]. However, these compounds did not show any promising value for further investigation (data not shown). Based on the concept of intermediate derivative method (IDM), which supposedly finds novel bioactive compound efficiently [26], we are trying to determine whether there is any benefit of fluorination on quercetin due to that fluorinated compounds have become very successful chemical entities for clinical application [27–29]. There are no reports regarding the fluorination of quercetin. In this study, we are trying to enhance its bioactivity by chemical modification using fluorination approach to obtain novel chemical entities. The compound we synthesized is named 8-trifluoromethyl-3,5,7,3',4'-O-pentamethyl-quercetin (TFQ) and was evaluated its antitumor activities and molecular mechanisms.

In a previous study, we elucidated that quercetin activates AMPK pathway which may be a major mechanism for its unique anticancer effects [30]. AMPK is a metabolic sensor in the cell activated by a high AMP: ATP ratio and low nutrient availability and signals to shut off anabolic processes such as protein synthesis in favor of catabolic processes such as fatty acid oxidation [31]. AMPK plays an important role in regulating cellular metabolism, preserving cellular energy homeostasis, and is also involved in many other cellular processes, including cell apoptosis [32, 33]. Recently, emerging evidence has implicated the potential roles of AMPK signaling in tumor initiation and progression [34]. Furthermore, AMPK has been considered as a potential therapeutic target for the treatment of cancer [35]. Activation of AMPK induces cell cycle arrest and inhibits cell survival in malignant cells through multiple mechanisms including up-regulation of the p53-p21 axis [36], and down-regulation of the mammalian target of rapamycin (mTOR) pathway [37, 38].

In our quest to develop novel quercetin derivatives with increased potency for AMPK activation and mTOR inhibition, we found that compared with quercetin, TFQ activated AMPK with significantly greater potencies. Therefore, it would be an attractive approach to develop novel AMPK activators as anti-cancer agents from structure-modified natural compound, which possess higher efficacy, lower toxicity.

RESULTS

Chemistry

The TFQ (3), a derivative of quercetin containing a trifluoromethyl group, was prepared by following the expected reaction route in Scheme 1. Thus, reaction of the commercially available quercetin with iodomethane afforded the known full methylated product (1) [39]. The product were iodinated with ICl in dry DMSO to yield compound 2 [40]. The product 2 was then reacted with the trifluoromethyl reagent (methyl fluorosulfonyldifluoroacetate) under nitrogen protection in the presence of CuI/DMF/HMPA afforded the desired compound 3 after purification by prep-HPLC [41]. Compound 3 was elucidated as 8-trifluoromethyl-3,5,7,3',4'-O-pentamethyl-quercetin by NMR and HRESIMS techniques. The NMR spectra of compound 3 were showed in Figures 1 and 2, and the NMR data of compounds 1, 2 were listed in supplemental materials.

TFQ inhibits bladder cancer cell survival

Three bladder cell lines (MB49, UMUC3, T24) were exposed to 0–160 μ M TFQ or quercetin (Que) to evaluate their inhibition on the survival. The results demonstrated that TFQ exerted more potent cytotoxic effects against MB49 (IC_{50} 44.69 μ M), UMUC3 (IC_{50} 72.65 μ M) and T24 (IC_{50} 100.46 μ M) cell lines compared to Que (IC_{50} 72.45, 94.69 and 118.91 μ M, respectively) (Table 1 and Figure 3A–3C) although the differences are mild. The survival of normal cells PEBC was not significantly inhibited when treated with TFQ for 48 h compared with Que, suggesting that TFQ had much less cytotoxic effect on normal cells than Que, as shown in Figure 3D.

TFQ suppresses colony formation

Colony formation was examined in the presence of TFQ or Que with the range of 0–40 μ M. As shown in Figure 4A–4C, colony numbers were significantly decreased in the three bladder cancer cells. The results confirmed the TFQ exerted a better suppression effect on bladder cancer cell survival or motility than Que in MB49 and UMUC3 cell lines but there was no significant difference in T24 cell line.

Table 1: Inhibitory concentration 50% (IC₅₀) of Que and TFQ

IC ₅₀ value	IC ₅₀ value	
	TFQ	Que
MB49	44.69	72.45
UMUC3	72.65	94.69
T24	100.46	118.91
PEBC	168.26	105.72

Scratch wound healing assay

Cell scratch assay was used to analyze whether TFQ or Que affected the migration of bladder cancer cells. As shown in Figure 5, at a low concentration of 2.5 μ M, cell free area of the TFQ-treated group was significantly wider than both the control and Que-treated groups in all three bladder cancer cell lines at 24 and 48 hours respectively. There was a dramatic difference in control and Que-treated groups of MB49 but there was no significant difference in T24, UMUC3. Similar pattern was observed in high concentration treated groups (In Supplementary Materials).

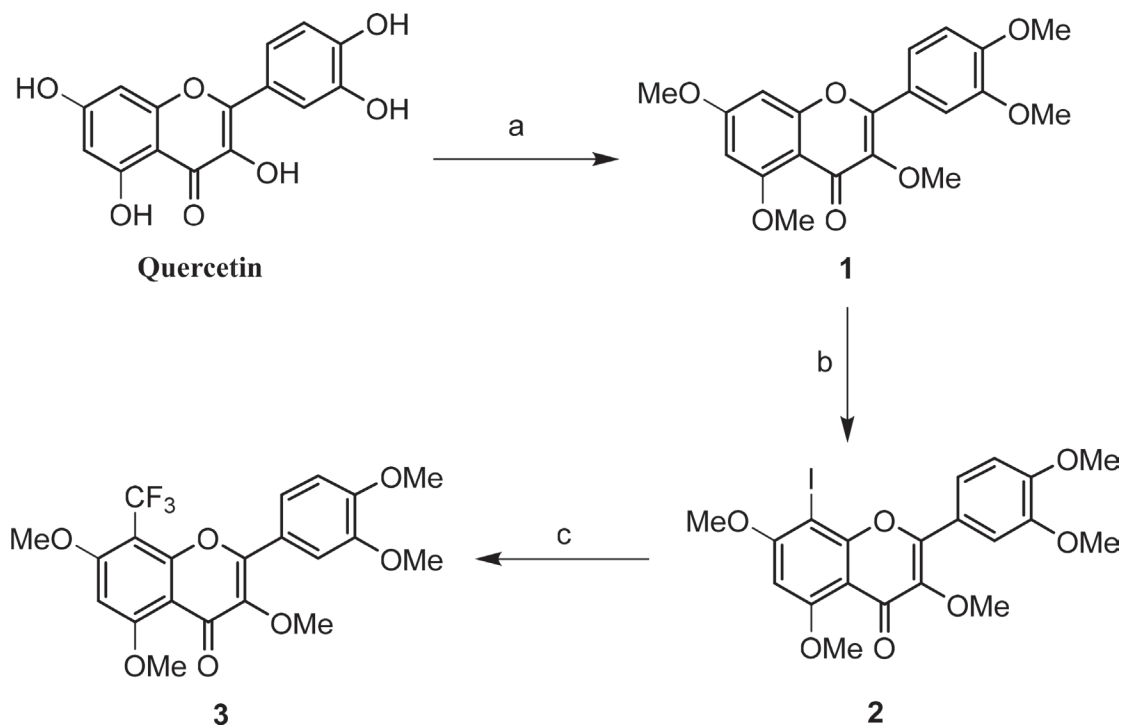
Effects on apoptosis with treatment of TFQ

Our previous studies have shown that quercetin can induce apoptosis [30]. We next examined whether TFQ could induce apoptosis as well. Two human bladder cancer cell lines and one murine bladder cancer cell line were

treated with TFQ (0, 40 μ M, 80 μ M, 160 μ M) for 24 h and apoptosis was measured by Annexin V/PI staining. In this experiment, we found that TFQ led to a dose-dependent cell apoptosis. As shown in Figure 6, cellular apoptosis was considerably increased in the TFQ-treated groups compared to the control group in a dose-dependent manner. After treatment with 160 μ M TFQ, the apoptotic populations increased as follows: from 7.6% to 49.8% in MB49 cell line, from 11.% to 29.6% in UMUC3 cell line, and from 9.6% To 20.5% in T24 cell line. These results demonstrated that TFQ is able to induce apoptosis in bladder cancer cells.

TFQ activates AMPK

AMPK, a central energy sensor, is known as a crucial sensor in controlling metabolism and cancer cell growth. Previous study has elucidated that quercetin activates AMPK pathway which may be a major mechanism for



Scheme 1: Synthetic route of TFQ (3): (a) K₂CO₃, CH₃COCH₃, CH₃I, reflux; (b) ICl, AcOH/DMSO, 55°C; (c) FSO₂CF₂CO₂Me, CuI, HMPA/DMF, 75°C.

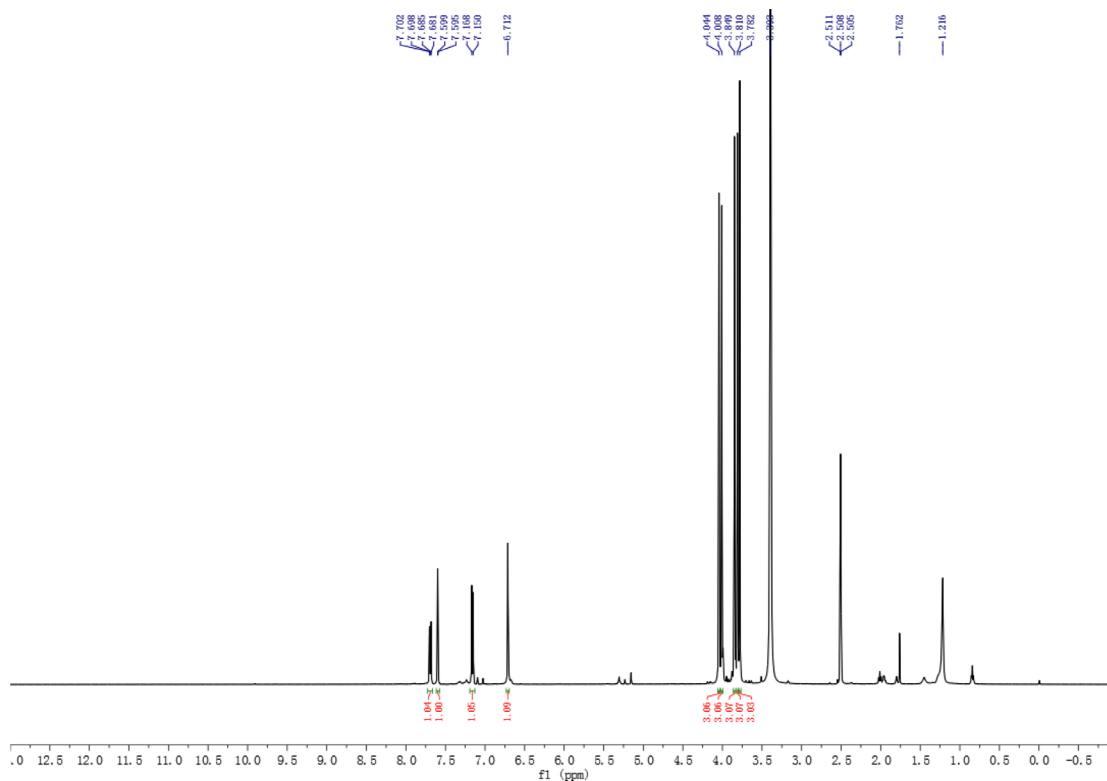


Figure 1: ¹H NMR spectrum of compound 3.

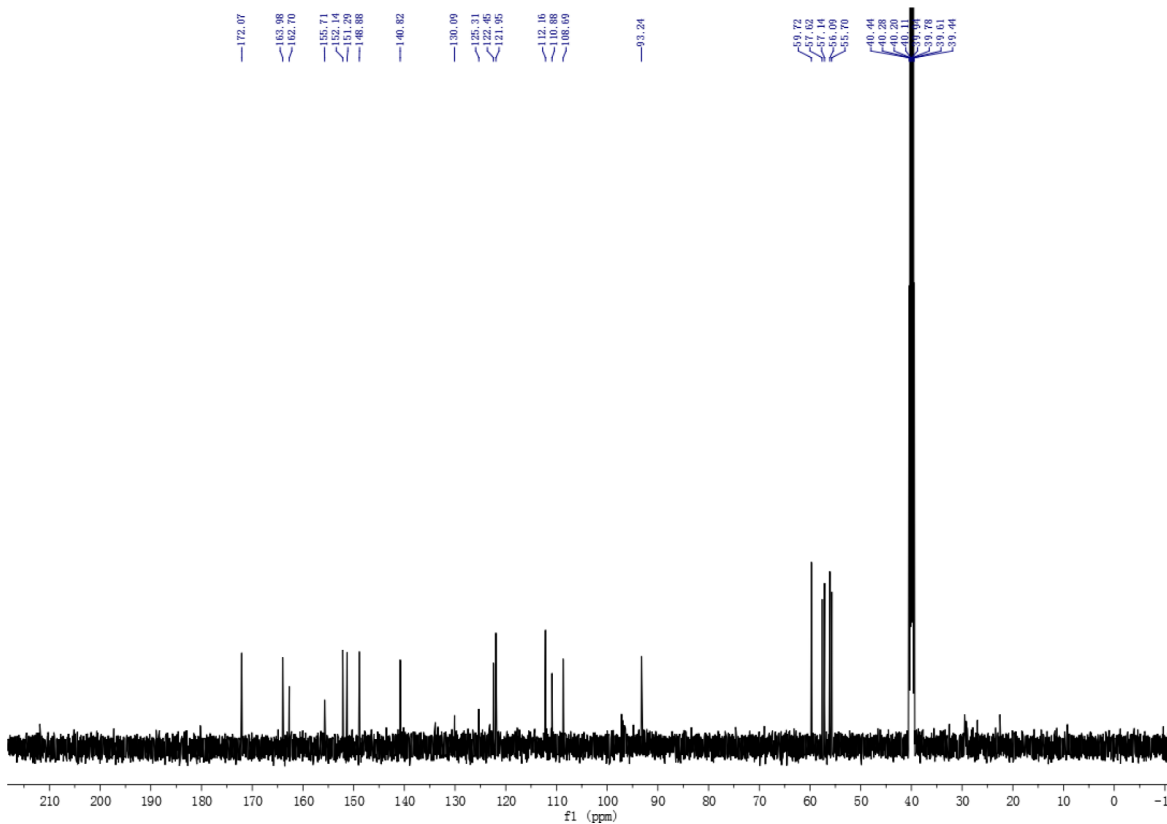


Figure 2: ¹³C NMR spectrum of compound 3.

its unique anticancer effect [30]. We compared the effects of TFQ and Que in this regard. Three bladder cancer cell lines (MB49, UMUC3 and T24) were treated with TFQ or Que with same dose in the range of 0-20 μM for 2 h, and cell lysates were analyzed for their levels of p-AMPK (T172), p-mTOR (S2448) and the mTOR downstream effectors p70S6K and p4EBP1 by Western blot analysis. The results revealed that TFQ activates AMPK with significantly greater potencies than Que as shown in Figure 7A–7F. This suggests that TFQ might enhance the pharmacological activities of Que with the activation of AMPK and influence on AMPK downstream. There was significant difference in the inhibitory effect of mTOR downstream effectors 4EBP1 and p70S6K after treated TFQ or Que 2 hours.

Next, we utilized AMPK specific inhibitor compound C to determine whether activating AMPK signaling pathway is essential for TFQ to exert anti-tumor effect. As shown in Figure 7G, the ability of TFQ to inhibit MB49 cancer cell survival was reduced after been treated with compound C, implying the inhibition

of AMPK accelerates survival of cancer cells. Similar trends of human bladder cancer cells T24 and UMUC3 were observed as shown in Figure 7H–7I, consistent with colony formation results as shown in Figure 7K–7L.

DISCUSSION

Bladder cancer remains one of the main malignancies that affect the genitourinary tract [42]. Nowadays, chemotherapy is the main treatment but recurrence and metastasis are often seen in the clinic which is becoming the most common problem. Therefore, fairly amount of research groups are focusing on studying natural products, produced by secondary metabolism of plants, in an attempt to find new and better treatments to tumors. Quercetin, a widely distributing member of natural flavonoids, is well known for its anticarcinogenic potential. It has been reported that that quercetin possesses strong anticancer activities against a variety of cancer cell lines including solid cancer [11–18]. Further study by chemical modifications to increase its efficacy could

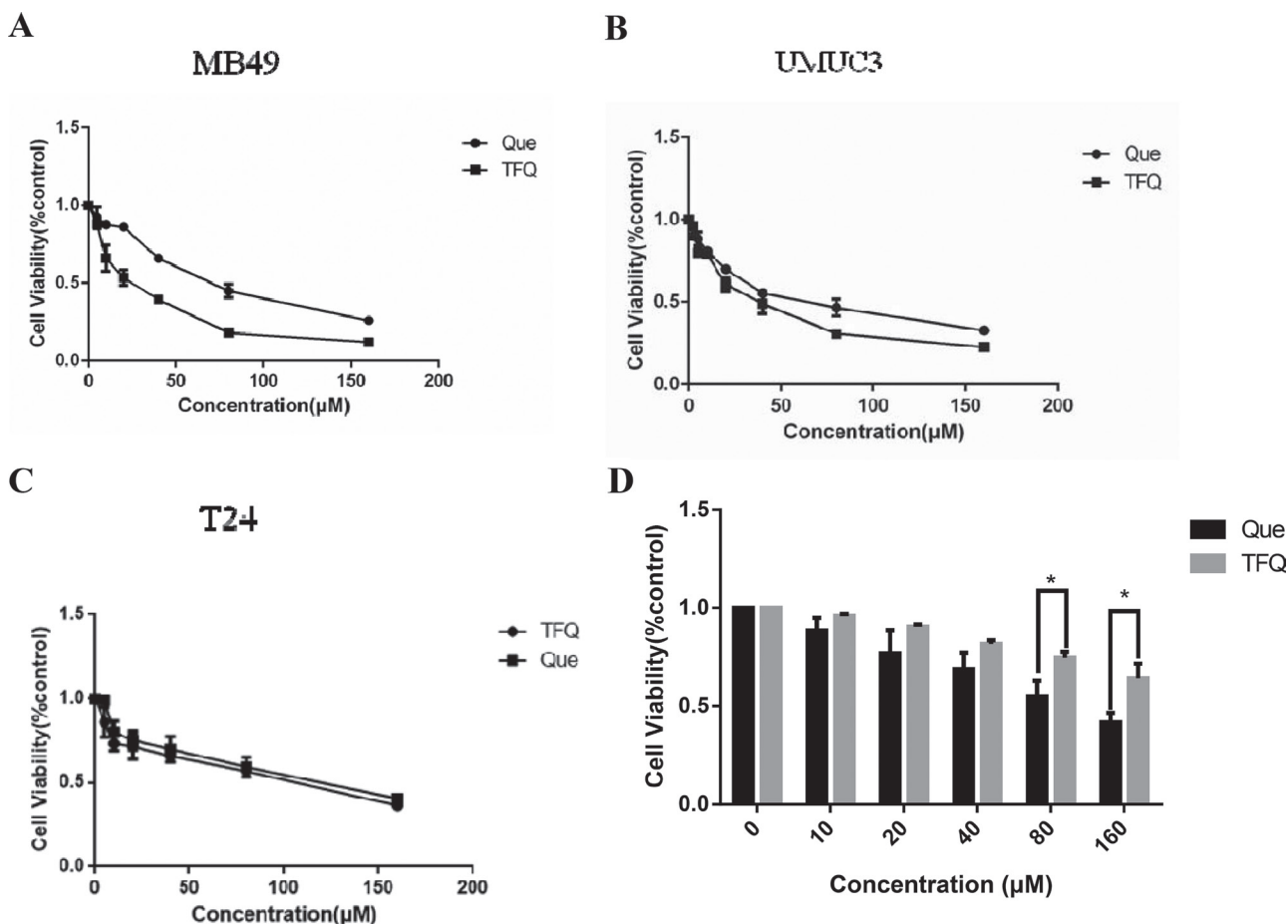


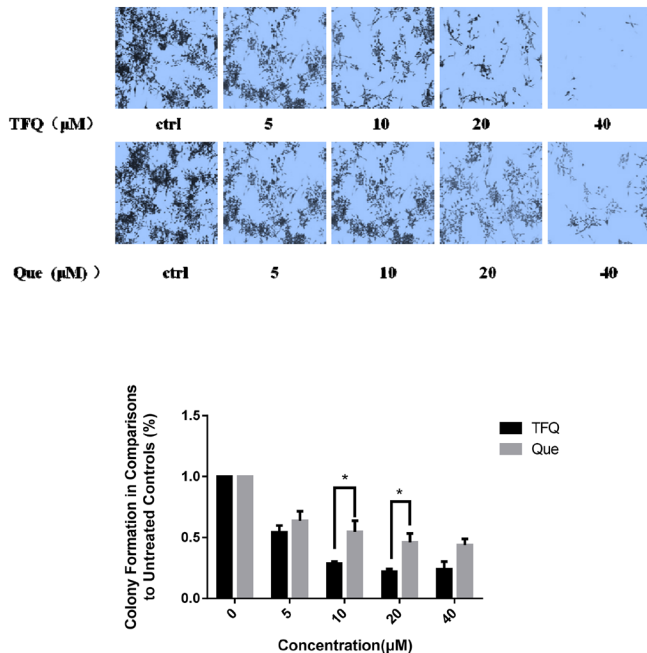
Figure 3: Treatment with Quercetin (Que) or TFQ on cell survival of 3 bladder cancer cell lines. (A) TFQ or Que inhibited MB49 survival synergistically. Cell viability was assessed after a 48 hour. Que or TFQ treatment at concentrations ranging from 0 to 160 μM using a tetrazolium-based assay. (B–C) TFQ or Que inhibited T24 and UMUC3 survival synergistically. Cell viability was assessed with 48 hour Que or TFQ at 0, 10, 20, 40, 80, 160 μM treatment in T24 and UMUC3, respectively. (D) TFQ or Que inhibited normal cell of PEBC survival synergistically. Results are presented as the median of 5 independent experiments.

further its applicability and discover more effective candidate molecules. It is well known that the introduction of CF₃ group into organic molecules often improves their physiological, physical chemical properties without

the introduction of extra steric hindrance. Moreover, trifluoromethylation frequently improve the bioactivity. So far, we have studied the trifluoromethylation of quercetin for the first time.

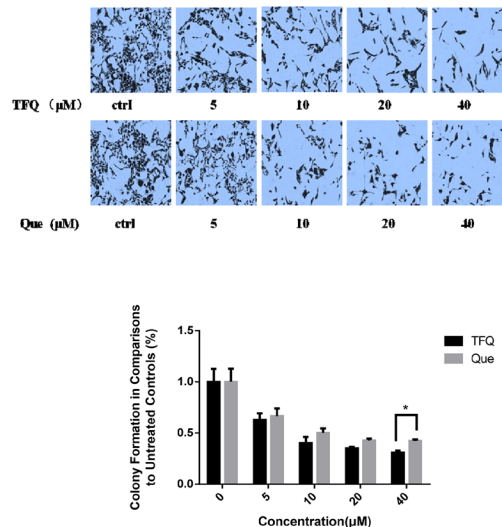
A

MB49



B

UMUC3



C

T24

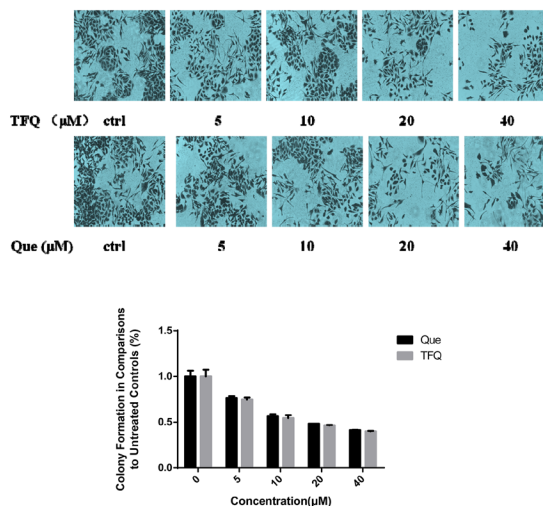


Figure 4: Evaluation of colony suppression of TFQ or Que on 3 bladder cancer cell lines. (A–C) clonogenic assay was assessed after 7 day TFQ or Que treatment and wells were stained with crystal violet at the end of the experiment. A. Clonogenic assay in MB49 was conducted with the assessed after 7 day treatment at various concentrations (0–40 μM) TFQ or Que. Above: The full view of wells were taken through stereomicroscope and images were taken through an inverted microscope with × 10 magnification. Below: the quantification of colony was determined by microplate area scan at OD 550 nm, Results are presented as the median of 5 independent experiments (Comparison was draw by the *t*-test (two-tailed). Data represent means ± SD; TFQ vs Que). (B–C) clonogenic assay was conducted with the treatment at various concentrations (0–40 μM) TFQ or Que in T24 and UMUC3, respectively. the full view of wells and their quantification were obtained through the same method as described in MB49. Results are presented as the median of 5 independent experiments (**P* < 0.05, TFQ vs Que).

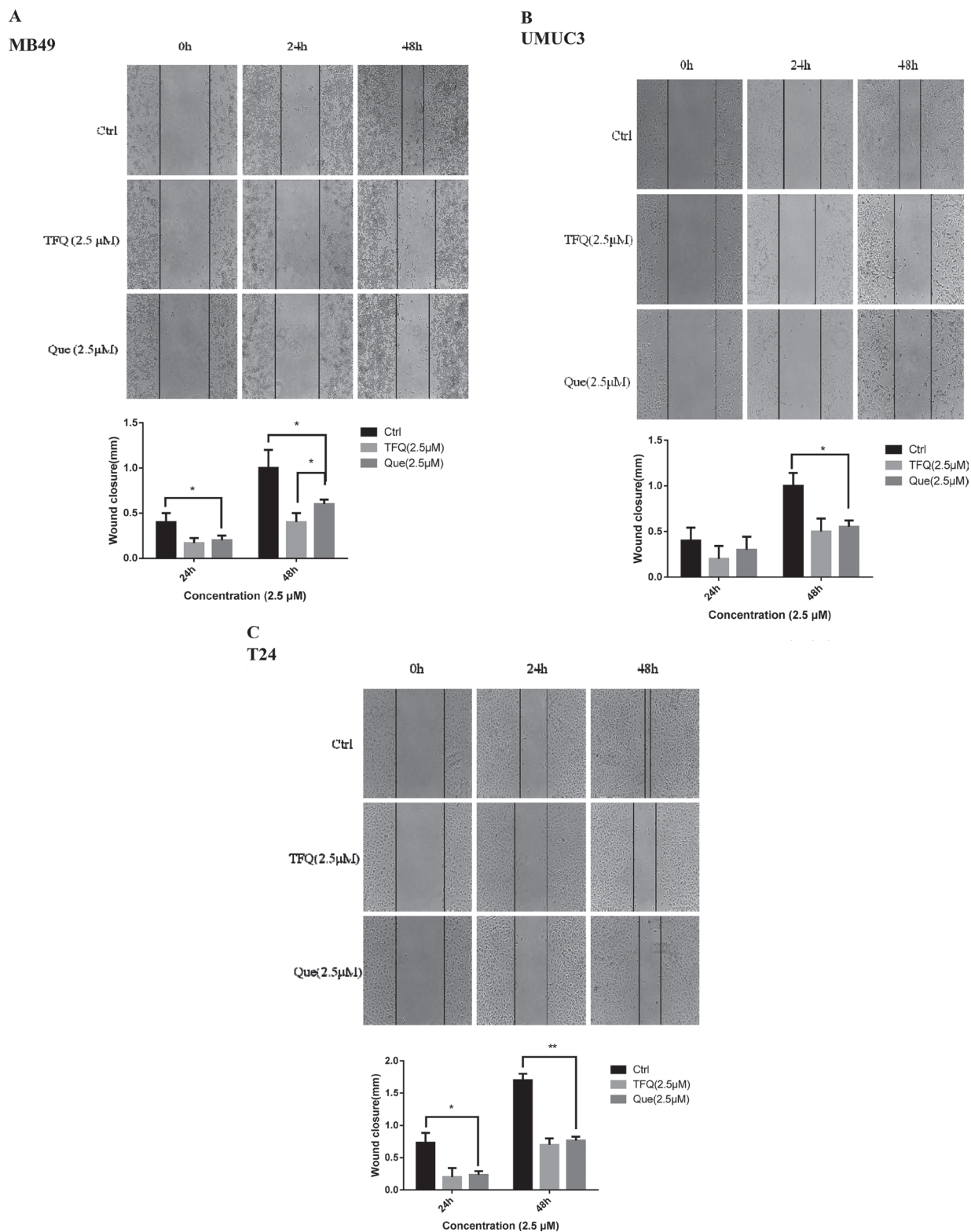


Figure 5: TFQ or Que treatment showed impaired migration in wound healing assays. (A–C) Images showed the gap of the scratched region of different cells with various treatments; A. Wound healing assays in MB49 conducted with the treatment of 5 μ M TFQ or Que. Above: The images were taken through an inverted microscope with $\times 10$ magnification. Below: The mean area was calculated using Image J software. Results are presented as the median of 5 independent experiments (* $P < 0.05$ vs control and TFQ vs Que). (B–C) Wound healing assays was conducted with the treatment at 2.5 μ M TFQ or Que in T24 and UMUC3, respectively. The images and their mean area were obtained through the same method as described in MB49.

The present study reported the synthesis of a novel trifluoromethylated derivative of quercetin, named TFQ. Previously, we reported that quercetin induced bladder cancer cells apoptosis by activation of AMPK signaling pathway [30]. Although the precise underlying mechanism(s) have not yet been fully elucidated, increasing evidence indicates that the P13K/Akt/mTOR pathway plays a crucial role in the survival and survival of cancer cells [43, 44]. Interestingly, compared with Que, TFQ activated AMPK and inactivated mTOR with significantly greater potencies in all of the tested bladder cancer cell lines. Accumulating evidence indicates that AMPK activation strongly suppresses cell survival, and further confirmed by AMPK inhibitor compound C. It has been proved that AMPK phosphorylation can induce TFQ-induced cell viability inhibition and inhibits bladder cancer progression. This is shown by colony formation assays, wound healing assays and apoptosis. Notably,

TFQ displays low cytotoxicity to human bladder normal cells. In conclusion, we herein confirm that the fluorinated quercetin derivative, TFQ blocks bladder cancer cells growth and increases apoptotic progression more effective than Que via activating AMPK and blocking the mTOR pathways. TFQ may be a useful small molecule candidate for the treatment of bladder cancer via AMPK/mTOR signaling pathway.

MATERIALS AND METHODS

Chemistry: general

Iodomethane was from Xiya Reagent. Methyl fluorosulfonyldifluoroacetate (FSO₂CF₂CO₂Me) and Iodine monochloride (ICl) was from Macklin Biochemical technology co., Ltd. Hexamethylphosphoramide (HMPA) and Copper(I) iodide were from aladding Biochemical

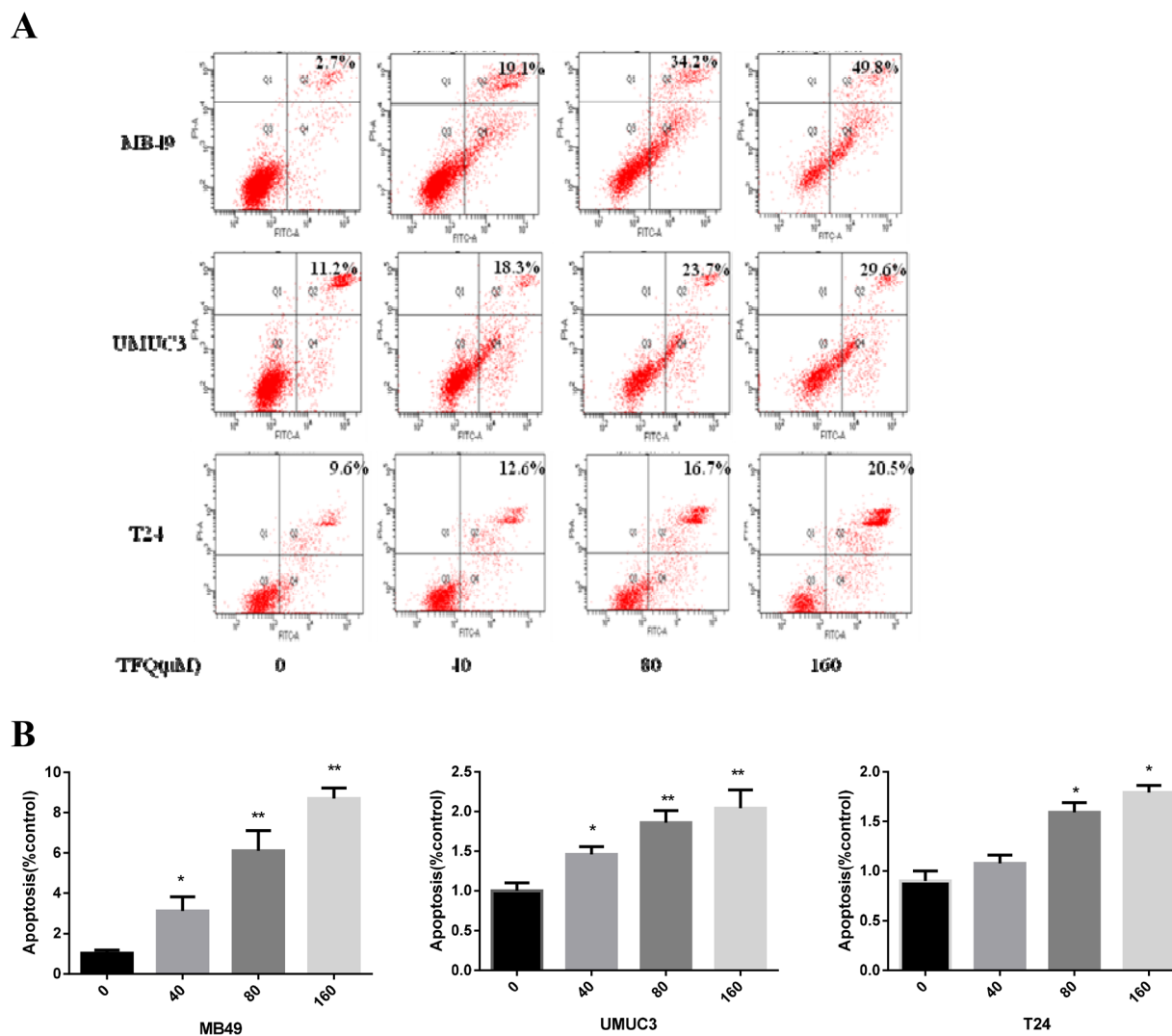
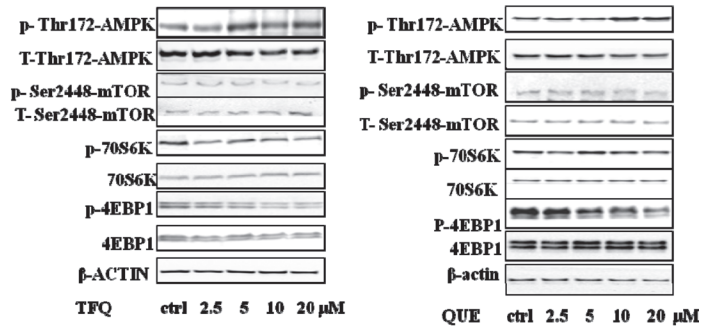
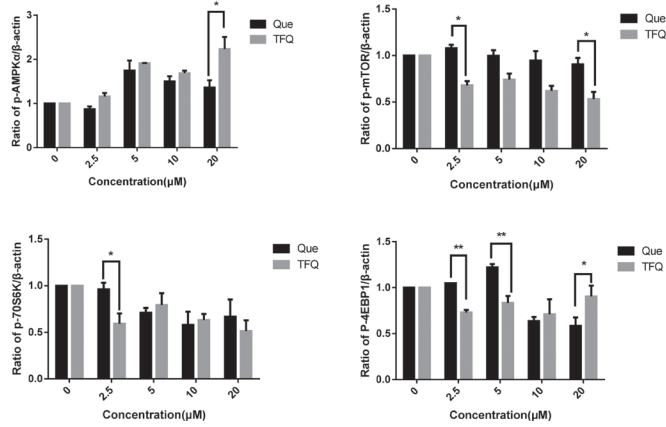


Figure 6: TFQ induces apoptosis in bladder cancer cell lines in a dose dependent manner. (A) Representative flow cytometry scatter plots of propidium iodide (PI) (Y axis) vs Annexin V-fluorescein isothiocyanate (FITC) (X axis). (B) Bar chart shows quantitative data of average of 3 independent flow cytometry experiments * $P < 0.05$, ** $P < 0.01$ compared with control.

A
MB49

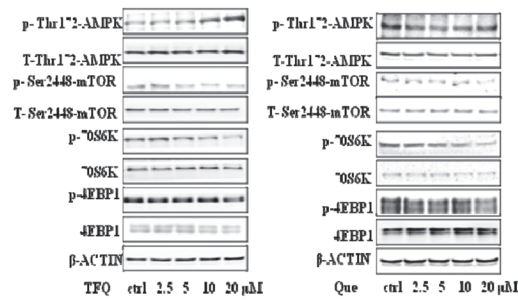


B

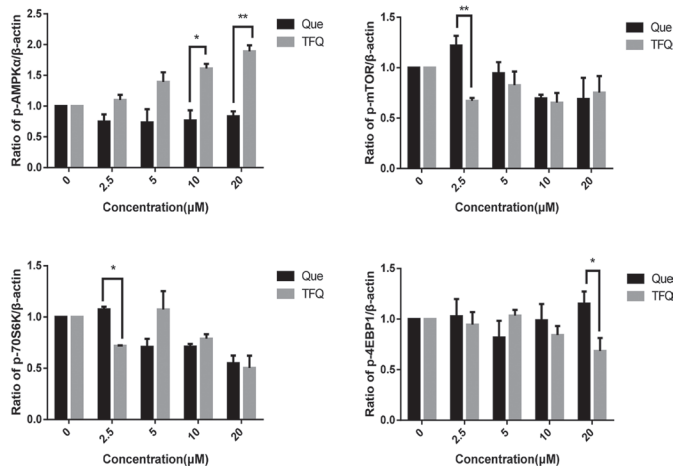


C

UMUC3

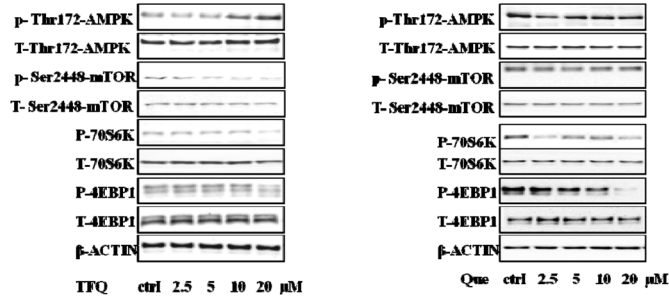


D

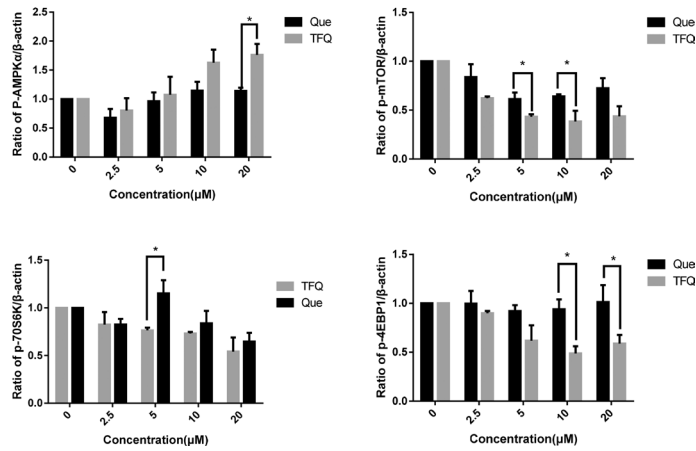


E

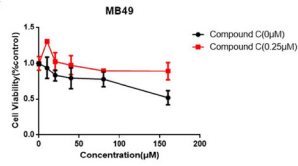
T24



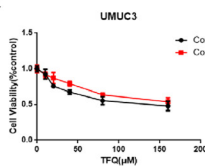
F



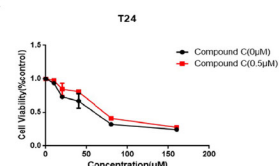
G



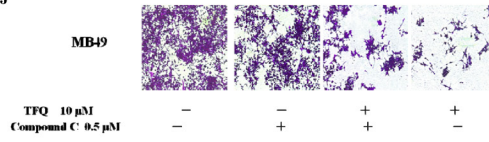
H



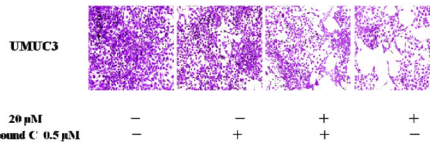
I



J



K



L

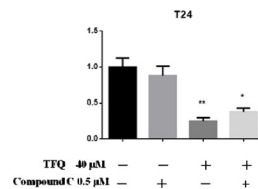
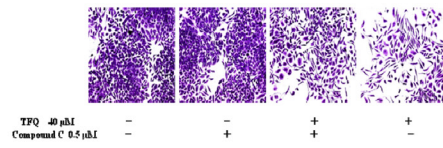


Figure 7: TFQ activates AMPK/mTOR intracellular signaling pathways at various concentrations. (A) Shows western blot of p-AMPK, p-p70S6K, p-mTOR, p-4EBP1, t-AMPK, t-mTOR, t-p70S6K and t-4EBP1 with the treatment of TFQ or Que (0–20 μ M) in MB49. β -actin was included as a loading control. (B) Shows the ratio of proteins of interests to β -actin calculated by the band density of western blots using Image J software of MB49 cell line. (* P < 0.05, ** P < 0.01 TFQ vs Que). Data were presented as cell survival curves. TFQ vs Que (C) Shows western blot results of p-AMPK, p-mTOR, p-P70S6K, p-4EBP1, t-AMPK, t-mTOR t-P70S6K and t-4EBP1 with the treatment of TFQ or Que (0–20 μ M) in UMUC3. (D) Shows the ratio of proteins of interests to β -actin calculated by the band density of western blots using Image J software of UMUC3 cell line. (* P < 0.05, ** P < 0.01 TFQ vs Que). (E) Shows western blot results of p-AMPK, p-mTOR, p-P70S6K, p-4EBP1, t-AMPK, t-mTOR t-P70S6K and t-4EBP1 with the treatment of TFQ or Que (0–20 μ M) in T24. (F) Shows the ratio of proteins of interests to β -actin calculated by the band density of western blots using Image J software of T24 cell line. (* P < 0.05, ** P < 0.01 TFQ vs Que). (G–I) Cell viability was assessed after 48 hour TFQ alone or TFQ combined with 0.25 μ M AMPK antagonist compound C treatment in MB49 and treatment at 20 μ M TFQ alone or TFQ combined with 0.5 μ M AMPK antagonist compound C in T24 and UMUC3, respectively. Results are presented as the median of 5 independent experiments. Compound C significantly reduced the decrease of cell survival and colony suppression caused by TFQ. (J–L) Clonogenic assay was assessed after 7 day TFQ treatment alone or combined with compound C and wells were stained with crystal violet at the end of the experiment. J. Clonogenic assay in MB49 was conducted with the treatment of 10 μ M TFQ, 0.25 μ M Compound C and their combination. (K–L) Clonogenic assay in MB49 was conducted with the treatment of 20 μ M TFQ, 0.5 μ M Compound C and their combination in UMUC3 and T24, respectively. Above: The full view of wells were taken through stereomicroscope and images were taken through an inverted microscope with \times 10 magnification. Below: the quantification of colony was determined by microplate area scan at OD 550 nm, Results are presented as the median of 5 independent experiments (Comparison was draw by the *t*-test (two-tailed). Data represent means \pm SD; * P < 0.05, ** P < 0.01 vs control).

technology co., Ltd. Anhydrous DMF was distilled under vacuum from CaH_2 . ^1H and ^{13}C NMR experiments were recorded on a Bruker AV-500 MHz spectrometer (Bruker, Karlsruhe, Germany) with tetramethylsilane (TMS) as the internal standard when $\text{DMSO-}d_6$ was used as a solvent. Chemical shifts are expressed in δ (ppm) and coupling constants (J) in Hz. High resolution (ESI) MS spectra were recorded using an Agilent 6550 iFunnel Q-TOF LC/MS system. Pre-HPLC experiments were conducted using an Agilent 1100 HPLC system and carried on preparative Sinochrom ODS-BP (10 μ m, 250 \times 10 mm, YiLiTe, Dalian, China). HPLC analysis was used to determine the purity (> 95%) of the compounds with a YMC Pack ODS-A (5 μ m, 250 \times 4.6 mm, YMC Co. Ltd, Kyoto, Japan) column.

Reagents

Quercetin was purchased from Aladdin chemistry Co. Ltd whereas TFQ was synthesized at our laboratory. Each compound was dissolved in DMSO to prepare a stock solution of 50 mM. Antibodies for the protein characterization were against total p70S6 kinase, phosphor-p70S6 kinase (Thr389), total AMPK, phosphor-AMPK (Thr172), phosphor-mTOR (S2448), total -mTOR, total 4E-BP1, phosphor-4EBP1(Thr-70) and β -actin were purchased from Cell Signaling Technology. Compound C was from Selleckchem (Houston, Texas, USA).

Synthesis

Synthesis of 2-(3,4-dimethoxyphenyl)-3,5,7-trimethoxy-4H-chromen 4-one (1)

A solution of quercetin (1.51 g, 5 mmol) in mixture of anhydrous potassium carbonate and acetone (60 ml) was heated and stirred at 70°C for 30 min and then the reaction mixture was cooled to room temperature (RT). A solution of CH_3I was added to the above mixture at room

temperature. The reaction mixture was then allowed to reflux at 70°C for 24 h until TLC showed that the reaction had been completed. The reaction mixture was poured into acidic water and filtered to obtain the precipitation after washing with H_2O three times. The products was recrystallized from ethanol to give the pure compound (1). Yellow solid, yield 1.23 g (66.1%); ^1H NMR (500 MHz, $\text{DMSO-}d_6$) δ : 3.75 (3H, s), 3.84 (3H, s), 3.85 (3H, s), 3.86 (3H, s), 3.89 (3H, s), 6.48 (1H, d, J = 2.0 Hz), 6.82 (1H, d, J = 2.0 Hz), 7.13 (1H, d, J = 8.5 Hz), 7.63 (1H, d, J = 2.0 Hz), 7.67 (1H, dd, J = 8.5, 2.0 Hz); ^{13}C NMR (125 MHz, $\text{DMSO-}d_6$): 56.0, 56.1, 56.4, 56.5, 59.7, 93.4, 96.3, 108.8, 111.4, 111.9, 121.8, 122.9, 140.8, 148.8, 151.1, 152.1, 158.6, 160.7, 164.1, 172.6.

Synthesis of 2-(3,4-dimethoxyphenyl)-8-iodo-3,5,7-trimethoxy- 4H-chromen-4- one (2)

A mixture of compound 1 (0.372 g, 1 mmol), ICl (0.485, 3 mmol) and glacial acetic acid (0.5 ml) in DMSO (10 ml) was heated with stirring at 55°C for 24 h. Then the saturated $\text{Na}_2\text{S}_2\text{O}_3$ aqueous solution was added until the red disappeared. The resulting mixture was filtered to obtain the filtrate after washing with DMSO for three times. The filtrate was extracted with ethyl acetate until TLC showed that the no product in aqueous phase. The organic phase was washed with saturated brines, dried (anhydrous Na_2SO_4), and evaporated under reduced pressure to get crude product. It was further purified by prep-HPLC using ACN/ H_2O (40/60) as eluent to give compound 2. Pale yellow solid, yield 182 mg (36.5%); ^1H NMR (500 MHz, $\text{DMSO-}d_6$): 3.78 (3H, s), 3.85 (3H, s), 3.88 (3H, s), 3.94 (3H, s), 4.01 (3H, s), 6.66 (1H, s), 7.15 (1H, d, J = 8.5 Hz), 7.88 (1H, d, J = 2.5 Hz), 7.88 (1H, dd, J = 8.5, 2.5 Hz); ^{13}C NMR (125 MHz, $\text{DMSO-}d_6$): 56.1, 56.2, 56.8, 57.6, 59.6, 65.4, 93.1, 109.2, 111.4, 112.1, 122.2, 122.9, 140.6, 149.0, 151.2, 152.0, 156.2, 161.8, 163.0, 172.4; HRESIMS calcd for $(\text{C}_{20}\text{H}_{19}\text{IO}_7 + \text{H})^+$ 499.0254, found 499.0252.

Synthesis of 2-(3,4-dimethoxyphenyl)-3,5,7-trimethoxy-8-(trifluoromethyl)-4H-chromen-4-one (3)

A solution of compound 2 (0.15 g, 0.3 mmol), CuI (37 mg), HMPA (0.3ml) in anhydrous DMF (30 ml) was heated with stirring at 75°C under strict water-free condition and nitrogen protection and then added the mixture of FSO₂CF₂CO₂Me (3 ml) and anhydrous DMF (20 ml) by dripping slowly. After dripped off, the reaction mixture continue to react with stirring at 75°C overnight. The solution was cooled to RT and then added saturated NH₄Cl aqueous solution to Quench the reaction. The reaction mixture was filtrated to remove the by-product. The filtrate was extracted with diethyl ether and wased washed 3 times with brine, dried (Na₂SO₄). The organic phase was evaporated to dryness in vacuo and the residue was purified by prep-HPLC using ACN/H₂O (40/60) as eluent to give compound 3. Pale yellow solid, yield 39 mg (29.5%); ¹H NMR (500 MHz, TMS): 3.78 (3H, s), 3.81 (3H, s), 3.84 (3H, s), 4.00 (3H, s), 4.04 (3H, s), 6.71 (1H, s), 7.16 (1H, d, *J* = 8.0 Hz), 7.60 (1H, d, *J* = 2.0 Hz), 7.69 (1H, dd, *J* = 8.0, 2.0 Hz); ¹³C NMR (125 MHz): 55.7, 56.0, 57.1, 57.6, 59.7, 93.2, 108.6, 110.8, 112.2, 122.0, 122.4, 125.3, 130.0, 140.8, 148.8, 151.3, 152.1, 155.7, 162.7, 164.0, 172.0; ¹⁹F NMR (471 MHz): -52.5; HRESIMS calcd for (C₂₁H₁₉F₃O₇ + H)⁺ 441.1161, found 441.1162.

Cell lines and culture conditions

Murine and human bladder cancer cell provided by Dr. P Guo (Institute of Urology, Xi'an Jiaotong University, Xi'an, Shanxi, China) was cultured in DMEM supplemented (Hyclone, Logan, UT, USA) with 10% of FBS (Hyclone, Logan, UT, USA) and 1% of penicillin-streptomycin at 37°C, in humidified air containing 5% of CO₂.

Cell viability assay

Cell viability was assessed using a tetrazolium based assay using microplate reader (Biotek, SYNERGY HTX, Vermont, USA). IC₅₀ values were determined through the dose-response curves.

Cells were seeded at 6 × 10³ per well in 96-well culture plates and incubated in medium containing 10% FBS. Different seeding densities were optimized at the beginning of the experiments. After 24 h, cells were treated with different concentrations of Que or TFQ (0, 5 μM, 10 μM, 20 μM, 40 μM, 80 μM, 160 μM) for 48 hours in incubator. 50 μl of MTT tetrazolium salt (Sigma) dissolved in Hank's balanced solution at a concentration of 2 mg/ml was added to each well with indicated treatment and incubated in CO₂ incubator for 5 h. Finally, the medium was aspirated from each well and 150 μl of DMSO (Sigma) was added to dissolve formazan

crystals and the absorbance of each well was obtained using a previously stated plate reader.

Clonogenic assay

Clonogenic survival was defined as the ability of the cells to form colonies. Images were taken and analyzed by microscopy (Leica, DFC450C, Wetzlar, Germany) and microplate reader (Biotek, SYNERGY HTX, Vermont, USA).

8 × 10³ cells were seeded into 24-well dishes in 0.5 ml of medium. Twenty-four hours later, cells were treated with different concentrations of Que or TFQ (0 μM, 2.5 μM, 5 μM, 10 μM, 20 μM), and then maintained for 6 days in a CO₂ incubator. Finally, the cells were fixed with 10% formaldehyde solution and then stained with 0.1% crystal violet, each experiment was performed in triplicate and colony numbers calculated through spectral scanning to determine the maximum absorption wavelength at 550 nm and measured its absorbance through area scanning. Statistical analysis was prepared with the GraphPad Prism 6.0. The Student's *t* test was used to compare colony numbers and determine the significance of these differences.

Measurement of cell migration

A total of 5 × 10³ cells were seeded onto a six-well plate and allowed to reach full confluence. The monolayer was wounded using a cocktail stick. Cells were incubated with serum-free DMEM medium, for the time period as stated. Digital images were taken at times 0, 24 h and 48 h. The mean area was calculated using Image J software. The experiments were repeated three times.

Assessment of apoptosis

Apoptosis was detected by flow cytometry via the examination of altered plasma membrane phospholipid packing by lipophilic dye Annexin V. Briefly, treated cells were harvested by trypsin, washed twice with PBS, and then resuspended in binding buffer at a concentration of 1 × 10⁶ cells/mL according to the manufacturer's instruction. Thereafter, 5 μL of Annexin V-FITC and 10 μL of propidium iodide were added into 100 μL of cell suspension and incubated for 30 minutes at room temperature in the dark. After adding 400 μL of binding buffer, labeled cells were counted by flow cytometry within 30 minutes. All early apoptotic cells (Annexin V-positive, propidium iodide-negative), necrotic/late apoptotic cells (double positive), as well as living cells (double negative) were detected by FACSC alibur flow cytometer and subsequently analyzed by Cell Quest software (Becton Dickinson). Argon laser excitation wavelength was 488 nm, whereas emission data were acquired at wavelength 530 nm

(FL-1 channel) for fluorescein isothiocyanate (FITC) and 670 nm (FL-3 c3 channel) for propidium iodide.

Protein characterization

Western blot assessment was performed using regular procedure. Primary antibody was added in BSA and allowed to incubate overnight at 4°C, washed with TBS/0.05% Tween-20 for 5 times (10 min per time) before the secondary antibody was added and then incubated for an additional hour at room temperature. The membrane was again washed 3 times before adding Pierce Super Signal chemiluminescent substrate (Rockford, IL, USA) and then immediately imaged on Chemi Doc (Bio-Rad, Hercules, CA, USA). The films were scanned using EPSON PERFECTION V500 PHOTO and quantified by Image J (NIH, Bethesda, MD, USA).

Statistical analysis

Statistical analysis was performed using SPSS 16.0 software. Student's *t* test was used to analyze the significance of two group results. Graphs were prepared using GraphPad Prism 6.0. All data are presented as mean ± SD. Statistical analyses were carried out using one-way ANOVA analysis and statistical significance was assumed at a value of **p* < 0.05, ***P* < 0.01.

ACKNOWLEDGMENTS AND FUNDING

This project was supported by Open Fund of National Laboratory of Subtropical Agriculture Ecology Process, Chinese Academy of Sciences (ISA2016204), Advanced Fund of Hunan Provincial Education Department (No. 15A117), Hunan Natural Science Foundation (2016JJ2187), Key Project of Hunan Province 2016 (2016JC2036), and National Key R&D Program (No. 2016YFD0501201), to X.Y and the National Natural Science Foundation of China (No. 31400311), the Program for Excellent Talents of Hunan Normal University (No. ET1508) to H. Z.

CONFLICTS OF INTEREST

None.

REFERENCES

1. Cancer facts & figures 2016; Atlanta (GA): American Cancer Society; 2016 [cited 2016 Aug 28].
2. Surveillance, Epidemiology, and End Results. SEER stat fact sheets: bladder cancer; Bethesda (MD): National Cancer Institute; 2016 [cited 2016 Aug 28].
3. Sternberg CN, Bellmunt J, Sonpavde G, Siefker-Radtke AO, Stadler WM, Bajorin DF, Dreicer R, George DJ, Milowsky MI, Theodorescu D. ICUD-EAU International Consultation on Bladder Cancer 2012: Chemotherapy for Urothelial Carcinoma—Neoadjuvant and Adjuvant Settings. *Oncol Rep.* 2013; 63:58.
4. Serretta V, Morgia G, Altieri V, Lallo AD, Ruggiero G, Salzano L, Battaglia M, Falsaperla M, Zito A, Sblendorio D. A 1-year maintenance after early adjuvant intravesical chemotherapy has a limited efficacy in preventing recurrence of intermediate risk non-muscle-invasive bladder cancer. *BJU Int.* 2010; 106:212–217.
5. Roupret M, Babjuk M, Comperat E, Zigeuner R, Sylvester RJ, Burger M, Cowan NC, Bohle A, Van Rhijn BW, Kaasinen E, Palou J, Shariat SF. European Association of Urology Guidelines on Upper Urinary Tract Urothelial Cell Carcinoma: 2015 Update. *Eur Urol.* 2015; 68:868–879.
6. Kaplan AL, Litwin MS, Chamie K. The future of bladder cancer care in the USA. *Nat Rev Urol.* 2014; 11:59–62.
7. Massari F, Ciccicarese C, Santoni M, Iacovelli R, Mazzucchelli R, Piva F, Scarpelli M, Berardi R, Tortora G, Lopez-Beltran A. Metabolic phenotype of bladder cancer. *Cancer Treat Rev.* 2016; 45:46–57.
8. Baig MA, Gawali VB, Patil RR, Naik SR. Protective effect of herbomineral formulation (Dolabi) on early diabetic nephropathy in streptozotocin-induced diabetic rats. *J Nat Med.* 2012; 66:500–509.
9. Cialdella-Kam L, Nieman DC, Sha W, Meaney MP, Knab AM, Shanelly RA. Dose-response to 3 months of quercetin-containing supplements on metabolite and quercetin conjugate profile in adults. *Br J Nutr.* 2012; 109:1–11.
10. Pinto SL, Kumar J, Partha G, Bechtol RA. Improving the economic and humanistic outcomes for diabetic patients: making a case for employer-sponsored medication therapy management. *Clinicoecon Outcomes Res.* 2013; 5:153.
11. Moon JH, Eo SK, Lee JH, Park SY. Quercetin-induced autophagy flux enhances TRAIL-mediated tumor cell death. *Oncol Rep.* 2015; 34:375.
12. Lv L, Liu C, Chen C, Yu X, Chen G, Shi Y, Qin F, Ou J, Qiu K, Li G. Quercetin and doxorubicin co-encapsulated biotin receptor-targeting nanoparticles for minimizing drug resistance in breast cancer. *Oncotarget.* 2016;7:32184–99. doi: 10.18632/oncotarget.8607.
13. Nwaeburu CC, Bauer N, Zhao Z, Abukiwan A, Gladkich J, Benner A, Herr I. Up-regulation of microRNA Let-7c by quercetin inhibits pancreatic cancer progression by activation of Numb1. *Oncotarget.* 2016;7:58367–58380. doi: 10.18632/oncotarget.11122.
14. Lagerweij T, Hiddingh L, Biesmans D, Crommentuijn MH, Cloos J, Li XN, Kogiso M, Tannous BA, Vandertop WP, Noske DP. A chemical screen for medulloblastoma identifies quercetin as a putative radiosensitizer. *Oncotarget.* 2016; 7:35776–35788. doi: 10.18632/oncotarget.7980.
15. He D, Guo X, Zhang E, Zi F, Chen J, Chen Q, Lin X, Yang L, Li Y, Wu W. Quercetin induces cell apoptosis of myeloma and displays a synergistic effect with dexamethasone

- in vitro* and *in vivo* xenograft models. *Oncotarget*. 2016; 7:45489–45499. doi: 10.18632/oncotarget.9993.
16. Braganhol E, Zamin LL, Canedo AD, Horn F, Tamajusuku AS, Wink MR, Salbego C, Battastini AM. Antiproliferative effect of quercetin in the human U138MG glioma cell line. *Anticancer Drugs*. 2006; 17:663.
 17. Ma L, Feugang JM, Konarski P, Wang J, Lu J, Fu S, Ma B, Tian B, Zou C, Wang Z. Growth inhibitory effects of quercetin on bladder cancer cell. *Front Biosci*. 2006; 11:2275–2285.
 18. Farias PF. Alterations in the extracellular catabolism of nucleotides are involved in the antiproliferative effect of quercetin in human bladder cancer T24 cells - Urologic Oncology: Seminars and Original Investigations. *Urol Oncol*. 2013; 31:1204.
 19. Brito AF, Ribeiro M, Abrantes AM, Pires AS, Teixo RJ, Tralhao JG, Botelho MF. Quercetin in Cancer Treatment, Alone or in Combination with Conventional Therapeutics? *Curr Med Chem*. 2015; 22:3025.
 20. Boers F, Lemiere G, Lepoivre JA, De Groot A, Dommissie R, De Bruyne T, Vlietinck AJ, Vanden Berghe DA. ChemInform Abstract: Synthesis and Antiviral Activity of 7-O-(ω -Substituted)-alkyl-3-O-methylquercetin Derivatives. *Pharmazie*. 1998; 53:512–517.
 21. Mattarei A, Biasutto L, Rastrelli F, Garbisa S, Marotta E, Zoratti M, Paradisi C. Regioselective O-derivatization of quercetin via ester intermediates. An improved synthesis of rhamnetin and development of a new mitochondriotropic derivative. *Molecules*. 2010; 15:4722–4736.
 22. Helgren TR, Sciotti RJ, Lee P, Duffy S, Avery VM, Igbinoba O, Akoto M, Hagen TJ. The synthesis, antimalarial activity and CoMFA analysis of novel aminoalkylated quercetin analogs. *Bioorg Med Chem Lett*. 2015; 25: 327–332.
 23. Zhou J, Wang LF, Wang JY, Tang N. Synthesis, characterization, antioxidative and antitumor activities of solid quercetin rare earth (III) complexes. *J Inorg Biochem*. 2001; 83:41–48.
 24. Leopoldini M, Russo N, Chiodo S, Toscano M. Iron chelation by the powerful antioxidant flavonoid quercetin. *J Agric Food Chem*. 2006; 54:6343–6351.
 25. Peng M, Liu F, Feng X, Yang F, Yang X. Synthesis of Brominated Quercetin Derivatives Using Distinct Brominating Systems. *Asian J Chem*. 2014; 26:4701–4703.
 26. Guan A, Liu C, Yang X, Dekeyser M. Application of the Intermediate Derivatization Approach in Agrochemical Discovery. *Chem Rev*. 2014; 114:7079–7107.
 27. Wang J, Sánchezroselló M, Aceña JL, Del PC, Sorochinsky AE, Fustero S, Soloshonok VA, Liu H. Fluorine in pharmaceutical industry: fluorine-containing drugs introduced to the market in the last decade (2001–2011). *Chem Rev*. 2014; 114:2432–2506.
 28. Gillis EP, Eastman KJ, Hill MD, Donnelly DJ, Meanwell NA. Applications of Fluorine in Medicinal Chemistry. *J Med Chem*. 2015; 58:8315–8359.
 29. Zhou Y, Wang J, Gu Z, Wang S, Zhu W, Aceña JL, Soloshonok VA, Izawa K, Liu H. Next Generation of Fluorine-Containing Pharmaceuticals, Compounds Currently in Phase II–III Clinical Trials of Major Pharmaceutical Companies: New Structural Trends and Therapeutic Areas. *Chem Rev*. 2016; 116:422.
 30. Su Q, Peng M, Zhang Y, Xu W, Darko KO, Tao T, Huang Y, Tao X, Yang X. Quercetin induces bladder cancer cells apoptosis by activation of AMPK signaling pathway. *Am J Cancer Res*. 2016; 6:498.
 31. Faubert B, Vincent EE, Poffenberger MC, Jones RG. The AMP-activated protein kinase (AMPK) and cancer: Many faces of a metabolic regulator. *Cancer Lett*. 2015; 356:165.
 32. Hardie DG, Alessi DR. LKB1 and AMPK and the cancer-metabolism link - ten years after. *BMC Biol*. 2013; 11:1–11.
 33. Liang J, Mills GB. AMPK: a contextual oncogene or tumor suppressor? *Cancer Res*. 2013; 73:2929.
 34. Cheng J, Zhang T, Ji H, Tao K, Guo J, Wei W. Functional characterization of AMP-activated protein kinase signaling in tumorigenesis. *Biochim Biophys Acta*. 2016; 1866:232.
 35. Hwang JT, Kwon DY, Yoon SH. AMP-activated protein kinase: a potential target for the diseases prevention by natural occurring polyphenols. *N Biotechnol*. 2009; 26:17–22.
 36. Rattan R, Giri S, Singh AK, Singh I. 5-Aminoimidazole-4-carboxamide-1-beta-D-ribofuranoside inhibits cancer cell survival *in vitro* and *in vivo* via AMP-activated protein kinase. *J Biol Chem*. 2005; 280:39582.
 37. Braganhol E, Zamin LL, Canedo AD, Horn F, Tamajusuku AS, Wink MR, Salbego C, Battastini AM. Antiproliferative effect of quercetin in the human U138MG glioma cell line. *Anticancer Drugs*. 2006; 17:663.
 38. Gwinn DM, Shackelford DB, Egan DF, Mihaylova MM, Mery A, Vasquez DS, Turk BE, Shaw RJ. AMPK phosphorylation of raptor mediates a metabolic checkpoint. *Mol Cell*. 2008; 30:214.
 39. Heijnen CG, Haenen GR, Vekemans JA, Bast A. Peroxynitrite scavenging of flavonoids: structure activity relationship. *Environ Toxicol Phar*. 2001; 10:199–206.
 40. Chaikovski VK, Kharlova TS, Filimonov VD, Saryucheva TA. ChemInform Abstract: Superactive Iodination Reagent on a Base of Iodine Chloride and Silver Sulfate. *Synthesis*. 1999; 1999:748–750.
 41. Chen QY, Wu SW. Methyl fluorosulphonyldifluoroacetate; a new trifluoromethylating agent. *J Electrochem Soc*. 1989; 705–706.
 42. Mori K, Enokida H, Kagara I, Kawakami K, Chiyomaru T, Tatarano S, Kawahara K, Nishiyama K, Seki N, Nakagawa M. CpG hypermethylation of collagen type I alpha 2 contributes to survival and migration activity of human bladder cancer. *Int J Oncol*. 2009; 34:1593–1602.

43. Alimova IN, Liu B, Fan Z, Edgerton SM, Dillon T, Lind SE, Thor AD. Metformin inhibits breast cancer cell growth, colony formation and induces cell cycle arrest *in vitro*. Cell Cycle. 2009; 8:909.

44. Gonzalezangulo AM, Mericbernstam F. Metformin: a therapeutic opportunity in breast cancer. Clin Cancer Res. 2010; 16:1695.